

Dimension reduction and global sensitivity metrics using active subspaces for coupled flow and deformation modeling

Hyunjung Lee and Elaine T. Spiller, Marquette University; Susan E. Minkoff*, the University of Texas at Dallas

SUMMARY

Accurate numerical simulation of complex hydraulic fracturing involves large numbers of model parameters. These parameters are uncertain as they are at best recorded in a few logged wells. Such simulations and subsequent estimation of microseismic events allow characterization of the nature and extent of the hydraulic fracture network. However, as one example of the way in which uncertainty affects our knowledge of the hydraulic fracturing process, errors in the microseismic event locations can be on the order of many meters. Moreover, estimating statistical uncertainty information about the output is computationally prohibitive for full multiphysics model simulations. To investigate new strategies for uncertainty quantification, we consider a simple model of two-way, loosely coupled single-phase fluid flow and linear elastic mechanical deformation. Loose coupling allows leveraging of significant development efforts common in more sophisticated flow and mechanics simulators. Active subspace strategies determine the most influential parameters in the model and rank these parameters in terms of their impact on simulator output. Once these parameters have been identified, inexpensive emulators which interpolate between simulation data points can be developed such as partial parallel emulators which can approximate spatially varying model output rapidly. In this study, two-way loose coupling uses fluid pressure output as a load on mechanical deformation, and updates for flow parameters such as porosity result from strain changes in mechanics. Our active subspace strategy finds that the coupling is essentially one way. Only the flow parameters impact the fluid pressure output whereas input parameters to both fluid flow and mechanics are important for the displacement. The emulator accurately interpolates the pressure and displacement data and will enable future studies that quantify the impact of uncertain input parameters and changing coupling terms (e.g. porosity) on the simulator output.

INTRODUCTION

Accurate numerical simulation of complex hydraulic fracturing involves large numbers of model parameters (McClure and Horne (2011); McChesney et al. (2016)). These parameters are often uncertain due to sparse geologic measurements recorded in a small number of wells in the field. This uncertainty in the subsurface description propagates beyond the fracture modeling itself into estimation of microseismic events which are important for characterizing the nature and extent of the hydraulic fracture network (Maxwell (2014); Kaderli et al. (2018, 2015)). Often these microseismic event locations are inaccurately estimated by tens of meters or more. To better numerically model such a complex process it is imperative that the simulation produces more than a single deterministic solution. Error bars or confidence intervals allow us to quantify the faith

we have in the simulation results. Unfortunately the curse of dimensionality severely restricts our ability to determine this statistical information for complex simulations. One method for estimating uncertainty is to determine which of the large number of model parameters has the most influence on the resulting solution or quantity of interest. Then a simpler surrogate or reduced order model can be used to develop statistical information about the solution by performing simulations using only these influential parameters (Smith (2013); Constantine (2015)). While the state of the art uncertainty quantification (UQ) strategies are in heavy use in fields such as climate modeling (Pachauri et al. (2014)) and some engineering applications, these techniques have not yet become common practice in the broader geoscience community. While there are few examples in the literature of applying these UQ ideas to exploration and production studies, Narasingham et al. (2017) use a global optimization algorithm applied to partition the time domain into clusters where snapshots contained within the cluster exhibit similar behavior. Then they apply a proper orthogonal decomposition to the solution snapshots within each cluster to capture the dominant spatial characteristics of the solution. The resulting basis functions allow them to derive ODE systems that are reduced models describing the dominant dynamics of the original nonlinear PDE's. They apply this idea to hydraulic fracture simulation but assume that the rock properties do not change with respect to time or space. In Siddhamshetty et al. (2018) the authors develop a new technique which integrates analytic models with data-based reduced order models for different parts of the hydraulic fracturing process.

Employing UQ strategies for multiphysics modeling (coupled process modeling) is a daunting challenge. As a first step towards the goal of understanding how best to quantify uncertainty for hydraulic fracturing, we examine a simpler model of coupled fluid flow and mechanical deformation, namely, 1D single-phase fluid flow and linear elastic deformation in a vertical column of mud (Terzaghi and Peck (1948); Minkoff and Kridler (2006)). We make use of a loose coupling algorithm that is relevant whenever one wants to leverage significant development efforts that have gone into sophisticated numerical simulation codes without having to resort to numerous simplifying assumptions required of fully coupled models (see Dean et al. (2003); Minkoff et al. (2003, 2004); Kim et al. (2011)). Specifically in this work we use two-way loose coupling to simulate fluid flow for a fixed set of times, passing the change in pore pressure to the mechanical deformation simulator. The mechanics code uses this pressure change as a load and outputs stresses and strains that lead to updated dynamic flow features (specifically porosity which changes due to compaction). This process then repeats for subsequent time steps. This model illustrates a key challenge: determination of influential input parameters and parameter-dependent features when these features can change during simulation. Active subspace strategies quantify which input parameters are the most influential and

Active subspace for dimension reduction

allow us to rank these influential parameters. For flow we find only the flow parameters seem to be influential while for mechanics both flow and deformation parameters are important. Developing a fast emulator allows us to determine statistical information about the output. Although initial porosity does not seem to impact the flow output, a dynamically changing porosity does.

THEORY AND METHODS

Background on Coupled Flow and Deformation Modeling

We investigate methods for analyzing uncertainty in the context of a simple 1D single-phase fluid flow and linear elastic deformation model. The model described below is given in detail in Minkoff and Kridler (2006) where various adaptive time stepping strategies are compared for loose 2-way coupling. We consider a thin body of soil, ie. a column of mud which is 100 inches high, confined by smooth, impermeable, rigid walls on all sides except the top surface. On the surface, perfect drainage is possible, and a load is applied suddenly to the column. The flow equation comes from conservation of mass and Darcy's Law and is given by

$$\rho_0 \frac{\partial(\phi p)}{\partial t}(x,t) = \frac{k}{\mu c} \frac{\partial^2 p}{\partial x^2}(x,t) \quad (1)$$

where we solve for the unknown pore pressure, p . The rate of flow is inversely proportional to the fluid viscosity, μ , and fluid compressibility, c . The permeability of the medium is given by k ; ρ_0 is initial fluid density, and ϕ is porosity.

For mechanical deformation we assume linear elasticity which relates stress, σ , to strain, ε , via Hooke's Law. Combining equilibrium equations for displacement with Hooke's Law results in the second-order differential equation for displacement in 1D:

$$-(\lambda + 2\hat{\mu}) \frac{d^2 u}{dx^2} = f. \quad (2)$$

Here u is the displacement, λ and $\hat{\mu}$ are the Lamé parameters that describe the solid material, and the one dimensional strain is defined as the derivative of displacement:

$$\varepsilon(u) = \frac{du}{dx}. \quad (3)$$

To loosely couple these two models, we will consider the change in pore pressure to be an external force for mechanics. Thus we augment the right hand side of Equation 2 as follows:

$$-(\lambda + \hat{\mu}) \frac{d^2 u}{dx^2} = f - \frac{dp}{dx}. \quad (4)$$

The resulting volume strain ε , calculated from solving Equation 4 and then post-processing via Equation 3, is used to update porosity for the next set of flow time steps. The porosity update formula is:

$$\phi(x,t) = 1 - \frac{(1 - \phi_0)}{e^\varepsilon}, \quad (5)$$

with ϕ_0 the initial porosity.

Active Subspaces: Overview

We begin by introducing the active subspace method for dimension reduction in mathematical models and for global sensitivity analysis. The active subspace description given here follows Constantine (2015).

Put simply, a subspace is a span of a set of vectors. In the active subspace method, one seeks to identify a few important vectors of the input parameters that capture most of the variability in the model response h . This is a two-step process. First one identifies these important combinations of input parameters. Second one calculates an *activity score* for each input parameter to rank the parameters in their order of influence on the model variability. In this context, the important parameters are the ones that, when perturbed, influence the model output more than others. In dynamical systems, the active subspace at multiple snapshots in time can be used to construct a dynamic active subspace (Loudon and Pankavich (2017)). In this work we consider the six input parameters for flow and deformation, namely, Young's modulus ($E = 10^8$ lb/in 2), Poisson's ratio ($\nu = 0.3$), permeability ($k = 1.86 \times 10^{-11}$ in/s), initial porosity ($\phi_0 = 0.6$), fluid compressibility ($c = 1.2 \times 10^{-8}$ psi), and fluid viscosity ($\mu = 5.6 \times 10^{-5}$ psi-s).

Let the model output h be a continuous function of the model input parameters, $\mathbf{x} \in \mathcal{X} \subseteq \mathbb{R}^m$, $h = h(\mathbf{x})$. We find the gradient of the model with respect to each input parameter

$$\nabla_{\mathbf{x}} h(\mathbf{x}) = \left[\frac{\partial h}{\partial x_1}(\mathbf{x}), \dots, \frac{\partial h}{\partial x_m}(\mathbf{x}) \right]^T, \quad (6)$$

and construct the $m \times m$ covariance-like matrix \mathbf{C} by taking the outer product of the gradient with itself and computing the average,

$$\mathbf{C} = \mathbb{E}_{\mathcal{X}} (\nabla_{\mathbf{x}} h)(\nabla_{\mathbf{x}} h)^T d\mathbf{x}. \quad (7)$$

Note that \mathbf{C} is an $m \times m$, positive semidefinite matrix, where m is the number of input parameters to $h(\mathbf{x})$. The eigendecomposition of \mathbf{C} is given by

$$\mathbf{C} = \mathbf{W} \Lambda \mathbf{W}^T, \quad \Lambda = \text{diag}(\lambda_1, \dots, \lambda_m), \quad \lambda_1 \geq \dots \geq \lambda_m \geq 0, \quad (8)$$

where \mathbf{W} is the $m \times m$ orthogonal matrix whose columns are the normalized eigenvectors of \mathbf{C} .

Discovering the Active Subspace

We can estimate the active subspace using the following procedure. For our loosely coupled model, we let $h(\mathbf{x}) = u(x,t;\mathbf{x})$ for displacement and $h(\mathbf{x}) = p(x,t;\mathbf{x})$ for pressure.

1. Sample the input parameter space globally by choosing N Latin Hypercube points in \mathcal{X} .
2. For each sample \mathbf{x}_j , evaluate $\nabla_{\mathbf{x}} h_j$. (We will do this twice for h , once for deformation and once for pressure.)
3. Approximate

$$\mathbf{C} \approx \hat{\mathbf{C}} = \frac{1}{N} \sum_{j=1}^N (\nabla_{\mathbf{x}} h_j)(\nabla_{\mathbf{x}} h_j)^T. \quad (9)$$

Active subspace for dimension reduction

4. Compute the eigendecomposition $\hat{\mathbf{C}} = \hat{\mathbf{W}}\hat{\Lambda}\hat{\mathbf{W}}^T$.

Since $\hat{\mathbf{C}}$ is positive semidefinite, it has a Cholesky decomposition, $\hat{\mathbf{C}} = \hat{\mathbf{G}}\hat{\mathbf{G}}^T$. Then the last step is equivalent to computing the singular value decomposition (SVD) of the matrix

$$\hat{\mathbf{G}} = \frac{1}{N} [\nabla_x h_1, \dots, \nabla_x h_N] = \hat{\mathbf{W}} \sqrt{\hat{\Lambda}} \hat{\mathbf{V}}. \quad (10)$$

The singular values are equivalent to the square root of the eigenvalues, and the left singular vectors are the eigenvectors.

We define the activity scores $\boldsymbol{\alpha}$ by,

$$\alpha_i = \sum_{j=1}^n \lambda_j w_{ij}^2, \quad i = 1, \dots, m, \quad (11)$$

where n is the dimension of the active subspaces (considering only λ_j above some small threshold) and w_{ij} is a component of the eigenvectors (Constantine and Diaz (2017)). The eigenvectors are weighted by the eigenvalues to capture the relative contribution of input parameters to the model response variability (Constantine and Diaz (2017)). The input parameters are then ranked by importance according to the values of $\boldsymbol{\alpha}$.

Active Subspaces: Numerical Results

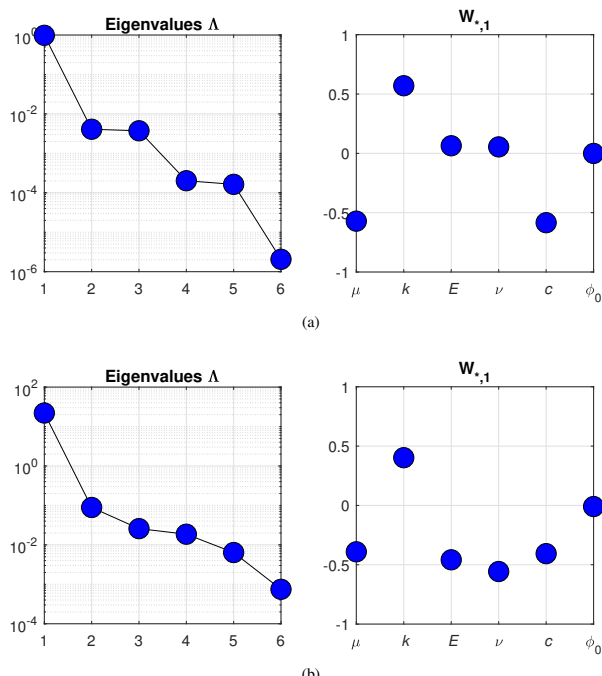


Figure 1: Eigenvalues of matrix C at 20 seconds and midway down the column (left) and the components of the first eigenvector corresponding to the first eigenvalue (right) in the (a) flow model and (b) deformation model.

We demonstrate dimension reduction and global sensitivity analysis using active subspaces. We approximate $\hat{\Lambda}$ and $\hat{\mathbf{W}}$ using gradients. Then, we (1) estimate the reduced input dimension via eigenvalue separation, and (2) calculate $\boldsymbol{\alpha}$ to rank the parameters by importance and identify parameters that are negligible in parameter studies. These results are summarized in Figure 1.

The simulation outputs u and p are evaluated at 100 Latin Hypercube points ($N = 100$) in 6-D input space ($m = 6$). The vertical column of mud has 100 grid points in depth, x , and we run 50 seconds of simulation time. The results below are for data at a single snapshot of time (time = 20 sec) and at a single point in space (depth = 50 in).

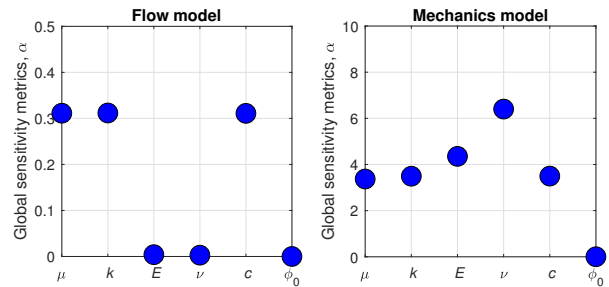


Figure 2: Global sensitivity metrics α computed using three active subspaces for the flow model (left) and five for the mechanics model (right).

The eigenvalues of the matrix \mathbf{C} (Λ) and the components of the eigenvector corresponding to the largest eigenvalue ($W_{*,1}$) are plotted in Figure 1. By identifying eigenvalues that fall within the first two clusters (before the second large gap), we can reduce the input dimensions to 3 active subspace dimensions ($n = 3$) in the flow model (Figure 1a), and 5 in the deformation model (Figure 1b). Activity scores $\boldsymbol{\alpha}$ are computed for each input parameter and are displayed in Figure 2.

The $\boldsymbol{\alpha}$ values are then used to rank the parameters' importance: $[k, \mu, c, E, \nu, \phi_0]$ in the flow model, and $[\nu, E, c, k, \mu, \phi_0]$ in the deformation model. The $\boldsymbol{\alpha}$ values suggest negligible ϕ_0 , ν and E in the flow model, resulting in a reduced input dimension of $m = 3$. Further, this indicates that variability in the flow model is *not* influenced by parameters in the mechanics model. In contrast, the mechanics model is most influenced by ν and E , but is still influenced by the flow parameters. This result suggests, in the context of uncertainty quantification, that the coupling is effectively one way from the flow model to the mechanics model.

Statistical Emulators: Background

Statistical emulators or surrogates are, simply, statistical models of complex physical models. One typically employs statistical emulators when the computational expense of exercising a physical model is high. Once a statistical emulator is constructed, evaluating it and approximating the true physical model is computationally “free”. Emulators are particularly useful if a large number of model evaluations are desired e.g. for numerical integration (including Monte Carlo), for MCMC simulations, for optimization, for validation, and for calibration (Smith (2013); Bayarri et al. (2007)). The advantage of using statistical emulators over other approximating schemes is that they interpolate the simulator output and offer a built-in mechanism to quantify the added uncertainty of utilizing an approximate model instead of the true model.

Often in uncertainty quantification the quantity of interest (QOI)

Active subspace for dimension reduction

is an integral of the form

$$E[Y] = \int g(\mathbf{x}) p(\mathbf{x}) d\mathbf{x}, \quad Y = g(X), \text{ and } X \sim p(\mathbf{x})$$

where p is a probability distribution function describing uncertain parameters, and g is a user defined function. If g represents the output of a computational model, we just have the mean of the computational model under p . Other common choices for g are higher moments of the computer model, exceedance probabilities, etc. The roadblock in any of these choices is that one evaluation of g is an expensive computer model run. This expense motivates approximating the computer model (or functional of the computer model), and we will do so with Gaussian process emulators (GP) (Sacks et al. (1989); Santner et al. (2003); Rasmussen and Williams (2006)).

To begin, we will assume that our computer model output is a draw from a mean-zero Gaussian process. That is, $y(\mathbf{x}) = \mu(\mathbf{x}) + Z(\mathbf{x})$, where μ is a mean trend (typically taken to be constant or linear), $E[Z] = 0$, $Var[Z] = \sigma^2$, and the correlation $C(Z(\mathbf{x}), Z(\mathbf{x}'))$ is a function of the distance between \mathbf{x} and \mathbf{x}' (typical choices are the power exponential function or the Matérn covariance functions (Gneiting et al. (2010))). In the coupled flow-deformation model, we choose $N = 100$ design points to construct GP emulators. Then we fit the correlation function to the design points and resulting outputs by solving an optimization problem to find the “best” correlation lengths for each input dimension. Next, we calculate the correlation between all design points and store those in an $N \times N$ matrix \mathbf{R} . Likewise, we also calculate the correlation between an untested input value \mathbf{x}^* and each design point. We will call this N vector \mathbf{r} . At this point, we will take the output at design runs to be either the deformation $u(x, t; \mathbf{x})$ or pressure $(p(x, t; \mathbf{x})$ at a single depth and time, and denote this output by \mathbf{y}^M . We can now construct a predictive mean and standard error (Sacks et al. (1989)) to evaluate the GP at untested input values. These are given by

$$\hat{y}(\mathbf{x}^*) = \mu(\mathbf{x}^*) + \mathbf{r}^T \mathbf{R}^{-1} (\mathbf{y}^M - \mu(\mathbf{x}^*)), \quad \text{and}$$

$$s^2(\mathbf{x}^*) = \sigma^2 \left(1 - \mathbf{r}^T \mathbf{R}^{-1} \mathbf{r} - \frac{\mathbf{1}^T \mathbf{R}^{-1} \mathbf{1}}{\mathbf{1}^T \mathbf{R}^{-1} \mathbf{1}} \right)$$

respectively, where $\mathbf{1}$ is an N vector of ones. (Note, this construction was used to estimate deformation and pressure in the active subspace selection, and approximate gradients were obtained by taking finite differences of \hat{y} .)

Parallel Partial Emulation of Pressure and Deformation

In the GP construction above, the output is taken to be scalar, e.g. displacement or pressure at one depth and time. One could fit emulators at each depth/time point of interest, but this process becomes computationally unwieldy as an optimization problem is required to find the set of optimal correlation parameters corresponding to each depth/time point. Instead, to approximate the displacement, and pressure as a function of depth, we will utilize the parallel partial emulator of Gu and Berger (2016). The key idea is to find one common set of range parameters for all of the functional output. This approach has the added bonus of requiring only a single inverse of \mathbf{R} at only a modest computational expense over a scalar-output emulator.

We fit parallel partial emulators (PPE) to displacement and pressure at $t = 30$ s. To demonstrate performance of the PPE we perform leave-one-out experiments. Thus we use $N=99$ design points, fit the PPE and use the predictive mean of the PPE to approximate the left-out design point’s response. For both displacement and pressure the error displayed at the bottom of figure (3) are roughly three orders of magnitude less than the scale of the output. This small error demonstrates the potential for parallel partial emulation to be an effective tool for quantifying uncertainty in coupled subsurface flows.

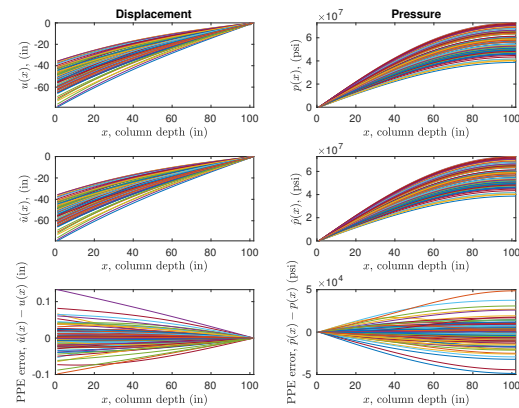


Figure 3: For both displacement (left) and pressure (right) we show output from the 100 design model runs (top), from the PPE estimates of each (middle), and the error between true model runs and the PPE (bottom).

CONCLUSIONS

Active subspaces reveal the important input parameters in each of our two models (fluid flow and mechanical deformation). Although we have a two-way coupled model, the flow model does not depend on the mechanics parameters. This result has interesting implications for uncertainty quantification – although the models and numerical computations are coupled via porosity, approximating the pressure is effectively independent from approximating the deformation. This decoupling can then be exploited in constructing statistical emulators that enable rapid uncertainty quantification studies on both average and extreme model behavior, and quantification of uncertainty during validation and calibration studies.

ACKNOWLEDGEMENTS

We would like acknowledge support of the ROMs working group of the MUMs 2018-2019 program at SAMSI, DMS-1638521. Spiller and Lee were further supported by NSF grants EAR-1521855 DMS-1622467 and DMS-1821338. Minkoff worked on this project during her sabbatical at SAMSI in Fall 2018 and acknowledges support from both SAMSI and UTD.

REFERENCES

- Bayarri, M. J., J. O., Berger, J., Cafeo, G., Garcia-Donato, F., Liu, J., Palomo, R. J., Parthasarathy, R., Paulo, J., Sacks, and D., Walsh, 2007, Computer model validation with functional output: Annals of Statistics, **35**, 1874–1906, doi: <https://doi.org/10.1214/009053607000000163>.
- Constantine, P. G., 2015, Active subspaces: Emerging ideas for dimension reduction in parameter studies: SIAM 2.
- Constantine, P. G., and P., Diaz, 2017, Global sensitivity metrics from active subspaces: Reliability Engineering and System Safety, **162**, 1–13, doi: <https://doi.org/10.1016/j.ress.2017.01.013>.
- Dean, R., X., Gai, C., Stone, and S., Minkoff, 2003, A comparison of techniques for coupling porous flow and geomechanics: Proceedings of the 17th Reservoir Simulation Symposium, SPE 79709.
- Gneiting, T., W., Kleiber, and M., Schlather, 2010, Matern cross-covariance functions for multivariate random fields: Journal of the American Statistical Association, **105**, 1167–1177, doi: <https://doi.org/10.1198/jasa.2010.tm09420>.
- Gu, M., and J. O., Berger, 2016, Parallel partial Gaussian process emulation for computer models with massive output: The Annals of Applied Statistics, **10**, 1317–1347, doi: <https://doi.org/10.1214/16-AOAS934>.
- Kaderli, J., M. D., McChesney, and S. E., Minkoff, 2015, Micro-seismic event estimation in noisy data via full waveform inversion: 85th Annual International Meeting, SEG, Expanded Abstracts, 1159–1164, doi: <https://doi.org/10.1190/segam2015-5867154.1>.
- Kaderli, J., M. D., McChesney, and S. E., Minkoff, 2018, A self-adjoint velocity-stress full waveform in-version approach to microseismic source estimation: Geophysics, **83**, no. 5, R413–R427, doi: <https://doi.org/10.1190/geo2017-0557.1>.
- Kim, J., H., Tchelepi, and R., Juanes, 2011, Stability, accuracy, and efficiency of sequential methods for coupled flow and geomechanics: SPE Journal, **16**, 249–262, doi: <https://doi.org/10.2118/119084-PA>.
- Loudon, T., and S., Pankavich, 2017, Mathematical analysis and dynamic active subspaces for a long term model of HIV: Mathematical Biosciences Engineering, **14**, 709–733, doi: <https://doi.org/10.3934/mbe>.
- Maxwell, S., 2014, Microseismic imaging of hydraulic fracturing: Improved engineering of unconventional shale reservoirs: SEG, Distinguished Instructor Short Course.
- McChesney, M. D., S. E., Minkoff, and G. A., McMechan, 2016, Rate and state flow and deformation simulation of microseismicity with elastic emission wavefield synthesis: 86th Annual International Meeting, SEG, Expanded Abstracts, 5055–5059, doi: <https://doi.org/10.1190/segam2016-13974653.1>.
- McClure, M. W., and R. N., Horne, 2011, Investigation of injection-induced seismicity using a coupled fluid flow and rate/state friction model: Geophysics, **76**, no. 6, WC181–WC198, doi: <https://doi.org/10.1190/geo2011-0064.1>.
- Minkoff, S., C., Stone, S., Bryant, and M., Peszynska, 2004, Coupled geomechanics and flow simulation for time-lapse seismic modeling: Geophysics, **69**, 200–211, doi: <https://doi.org/10.1190/1.1649388>.
- Minkoff, S., C., Stone, S., Bryant, M., Peszynska, and M., Wheeler, 2003, Coupled fluid flow and geomechanical de-formation modeling: Journal of Petroleum Science and Engineering, **38**, 37–56, doi: [https://doi.org/10.1016/S0920-4105\(03\)00021-4](https://doi.org/10.1016/S0920-4105(03)00021-4).
- Minkoff, S. E., and N. M., Kridler, 2006, A comparison of adaptive time stepping methods for coupled flow and de-formation modeling: Applied mathematical modelling, **30**, 993–1009, doi: <https://doi.org/10.1016/j.apm.2005.08.002>.
- Narasingham, A., P., Siddhamshetty, and J., Sang-II Kwon, 2017, Temporal clustering for order reduction of non- linear parabolic pde systems with time-dependent spatial domains: Application to a hydraulic fracturing process: AIChE Journal, **63**, 3818–3831, doi: <https://doi.org/10.1002/aic.v63.9>.
- Pachauri, R. K., M. R., Allen, V. R., Barros, J., Broome, W., Cramer, R., Christ, J. A., Church, L., Clarke, Q., Dahe, P., Dasgupta, N. K., Dubash, O., Edenhofer, I., Elgizouli, C. B., Field, P., Forster, P., Friedlingstein, J., Fuglestvedt, L., Gomez-Echeverri, S., Hallegatte, G., Hegerl, M., Howden, K., Jiang, B., Jimenez Cisneroz, V., Kattsov, H., Lee, K. J., Mach, J., Marotzke, M. D., Mastrandrea, L., Meyer, J., Minx, Y., Mulugetta, K., O'Brien, M., Oppenheimer, J. P., Pereira, R., Pichs-Madruga, G. K., Plattner, H. O., Pörtner, S. B., Power, B., Preston, N. H., Ravindranath, A., Reisinger, K., Riahi, M., Rusticucci, R., Scholes, K., Seyboth, Y., Sokona, R., Stavins, T. F., Stocker, P., Tschakert, D., van Vuuren, and J. P., van Ypersele, 2014, Climate change 2014: synthesis report. Contribution of Working Groups I, II and III to the fifth assessment report of the Intergovernmental Panel on Climate Change: IPCC.
- Rasmussen, C. E., and C. K., Williams, 2006, Gaussian processes for machine learning: The MIT Press.
- Sacks, J., W. J., Welch, T. J., Mitchell, and H. P., Wynn, 1989, Design and analysis of computer experiments: Statistical Science, **4**, 409–423, doi: <https://doi.org/10.1214/ss/1177012413>.
- Santner, T. J., B. J., Williams, and W. I., Notz, 2003, The design and analysis of computer experiments: Springer Science and Business Media.
- Siddhamshetty, P., K., Wu, and J. S.-I., Kwon, 2018, Optimization of simultaneously propagating multiple fractures in hydraulic fracturing to achieve uniform growth using data-based model reduction: Chemical Engineering Research and Design, **136**, 675–686, doi: <https://doi.org/10.1016/j.cherd.2018.06.015>.
- Smith, R. C., 2013, Uncertainty quantification: Theory, implementation, and applications: SIAM.
- Terzaghi, K., and R., Peck, 1948, Soil Mechanics in Engineering Practice: John Wiley and Sons.